Virology 386 (2009) 303–309

Contents lists available at ScienceDirect

Virology

journal homepage: www.elsevier.com/locate/yviro

N-terminal deletions of the øX174 external scaffolding protein affect the timing and fidelity of assembly

Asako Uchiyama [1], Peter Heiman, Bentley A. Fane *

Division of Plant Pathology and Microbiology, Department of Plant Sciences, University of Arizona, Tucson, AZ 85721, USA
The BIO5 Institute, University of Arizona, Tucson, AZ 85721, USA

ARTICLE INFO

Article history:
Received 4 October 2008
Returned to author for revision
25 November 2008
Accepted 24 January 2009
Available online 23 February 2009

Keywords:
Virus assembly
øX174
Microviruses
Scaffolding proteins

ABSTRACT

The first α-helices of *Microviridae* external scaffolding proteins function as coat protein substrate specificity domains. Mutations in this helix can lengthen the lag phase before progeny production. 5′ deletion genes, encoding N-terminal deletion proteins, were constructed on plasmids and in the øX174 genome. Proteins lacking the first seven amino acids were able to rescue a *nullD* mutant when expressed from a plasmid. However, the lag phase before progeny production was lengthened. The øX174 mutant with the corresponding genomic gene grew very poorly. The molecular basis of the defective phenotype was complex. External scaffolding protein levels were reduced compared to wild-type and most of the viral coat protein in mutant infected cells appears to be siphoned off the assembly pathway. Second-site suppressors of the growth defects were isolated and appear to act via two different mechanisms. One class of suppressors most likely acts by altering mutant external scaffolding protein expression while the second class of suppressors appears to act on the level of protein–protein interactions.

Introduction

The assembly of viral proteins and nucleic acids into a biologically active virion involves diverse and numerous macromolecular interactions, which are often mediated by scaffolding proteins (Fane and Prevelige, 2003; King and Casjens, 1974). While most viral scaffolding proteins are located inside procapsids, øX174 and some satellite phages also require an external scaffolding protein (Goldstein et al., 1974; Fane et al., 2006). Although both the external and internal scaffolding proteins are normally essential in these dual scaffolding systems, the external scaffolding proteins appear to be more critical for assembly. For example, P4 procapsid-like particles can be assembled *in vitro* using only the capsid and external scaffolding proteins (Wang et al., 2000), and a øX174 sextuple mutant strain can assemble without the internal protein (Chen et al., 2007).

The øX174 assembly pathway is illustrated in Fig. 1A. The first detectable assembly intermediates are pentamers of the major coat and major spike proteins, the respective 9S and 6S particles. Five internal scaffolding proteins bind to the underside of the 9S particle, a pentamer of coat proteins (Cherwa et al., 2008; Tonegawa and Hayashi, 1970). This induces a conformational change that enables the 9S* particle to interact with a pentamer of the major spike protein (6S particle), creating the 12S* assembly intermediate (Cherwa et al., 2008). 240 copies of the external scaffolding proteins then arrange twelve 12S* particles into procapsids (Dokland et al., 1999; Fane et al., 2006). The external scaffolding protein subunits are not arranged in a quasi-equivalent lattice (Dokland et al., 1999, 1997). Instead the proteins are arranged as two asymmetric dimers (D_1D_2 and D_3D_4), per asymmetric unit (Fig. 1B). Each subunit assumes a unique structure to mediate the required local contacts with the coat, neighboring external scaffolding, and major spike proteins.

The results of previous structure–function analyses conducted with chimeric external scaffolding proteins, in which the first α-helix of the øX174 external scaffolding protein was replaced with either helices from the related viruses α3 or G4 phage, indicate that this structure acts as a coat protein substrate specificity domain early in the morphogenetic pathway (Burch and Fane, 2000; Uchiyama et al., 2007; Uchiyama and Fane, 2005). The primary sequence of the first α-helices from the G4, α3 and øX174 external scaffolding proteins are depicted in Fig. 1C. The sequences of the α3 and øX174 proteins are highly diverged in this region, which most likely accounts for the inability of the α3/øX174 protein to recognize the øX174 coat protein (Burch and Fane, 2000). While the G4/øX174 protein could support assembly, the results of kinetic analyses demonstrated that a higher critical concentration of the chimeric protein was needed to nucleate a step in the assembly pathway, which was reflected in a longer lag phase before the rapid infectious progeny detection (Uchiyama et al., 2007).

With the exception of the first seven amino acids, the first helices of the G4 and øX174 proteins are relatively conserved. To further

* Corresponding author. The BIO5 Institute, Keating Building, University of Arizona, Tucson, AZ, 85721, USA. Fax: +1 520 621 6366.
E-mail address: bfane@u.arizona.edu (B.A. Fane).
[1] Present address: Department of Plant Pathology and Plant-Microbe Biology, Cornell University, Ithaca, NY, 14853, USA.

0042-6822/$ – see front matter © 2009 Elsevier Inc. All rights reserved.
doi:10.1016/j.virol.2009.01.030

investigate the role of the N-terminal amino acids during assembly, 5′-terminal deletion genes were constructed on plasmids and placed directly in the viral genome. The kinetics of phage growth and the assembly pathway were investigated. Like previously generated results with chimeric external scaffolding proteins, the results of the analyses presented here indicate that the N-terminal amino acids affect the timing of progeny production and morphogenetic fidelity.

Results

N-terminal deletions of the øX174 external scaffolding protein alter the timing of progeny production

N-terminal deleted proteins were initially expressed from plasmids and assayed for the ability to complement a *nullD* allele. The results of those experiments indicated that the first seven amino acid residues of the protein were not essential for plaque formation. However, the deletion of the first nine amino acid residues resulted in the loss of complementation activity.

A previously characterized phage containing a G4/øX174 external scaffolding protein gene, in which the genetic material encoding the first α-helices of these two related viruses were interchanged, exhibited delayed assembly kinetics (Uchiyama et al., 2007; Uchiyama and Fane, 2005). The lag phase before particle production was lengthened. However, after the lag phase, progeny were rapidly produced at or near wild-type rates. To determine whether deletions in the first α-helix acted in a similar manner, the growth of a *nullD* mutant was examined in cells expressing the ΔD7, ΔD9, and wild-type proteins (Fig. 2A). In these and all kinetic experiments, infections were synchronized as described in Material and Methods and phage were pre-attached to cells. The lag phase before the appearance of progeny was lengthened in cells expressing the ΔD7 protein (circles) relative to the wild-type control (squares), and the overall yield was lower by an order of magnitude. No progeny were produced in cells expressing the ΔD9 protein (data not shown).

The phenotypes and growth kinetics of the øX174ΔD7 and ΔD9 strains

While the results of the cloned gene complementation tests are suggestive, the expression of proteins from high copy number plasmids leads to a protein pool at the onset of infection, which can shorten the lag phases or otherwise drive and facilitate reactions that may not occur under physiological conditions (Uchiyama et al., 2007; Uchiyama and Fane, 2005). Therefore, 5′ deletion genes were built directly into the øX174 genome. It was possible to build both the ΔD7 and ΔD9 5′ deletion genes without altering the stop codon of the upstream C gene, which overlaps with the first two codons of gene D, or the D protein primary structure after the deletion. However, a missense mutation had to be introduced in the penultimate codon of gene C to construct these strains, which conferred an S→H substitution in the C-terminal amino acid. The *øX174ΔD9* strain has an absolute lethal phenotype, only forming plaques in cells expressing the wild-type D protein. The *øX174ΔD7* strain was viable in the absence of exogenously expressed D protein at 33 °C but plaques size was very small and plating efficiencies

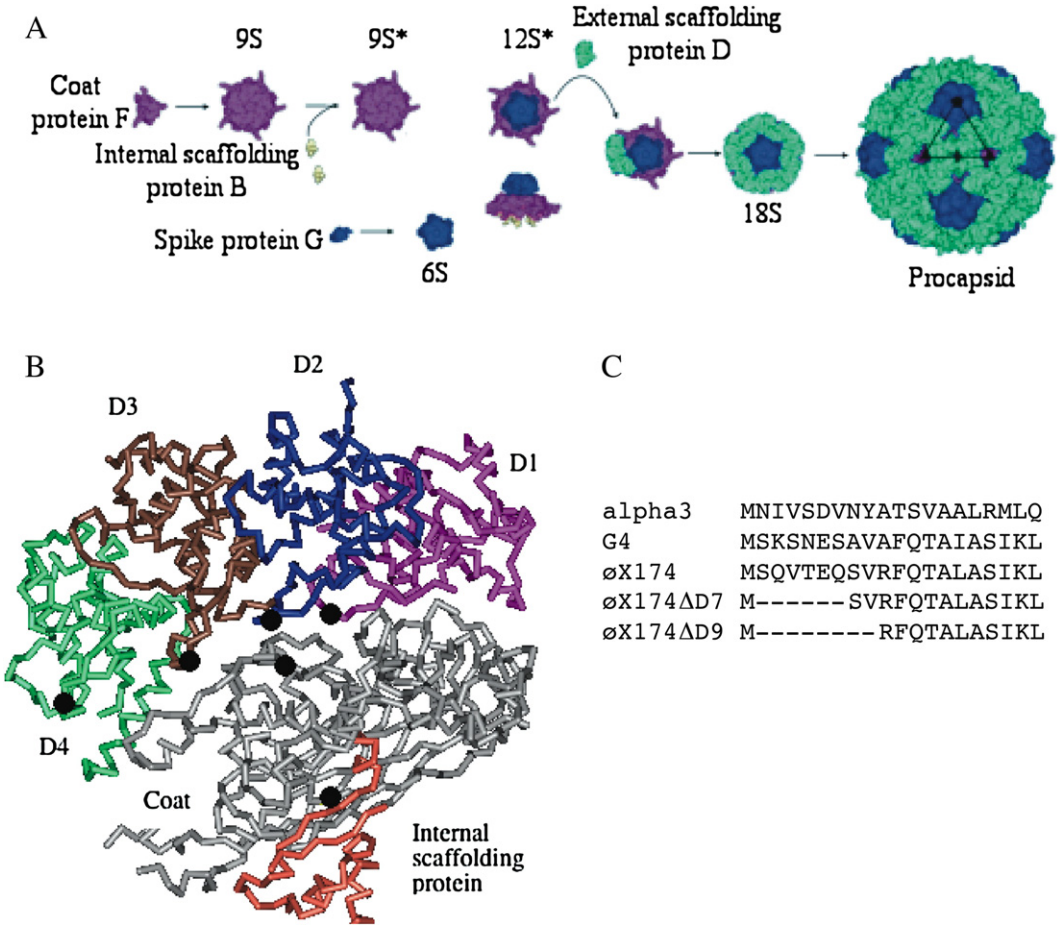

Fig. 1. (A) The øX174 morphogenetic pathway. (B) The four external scaffolding subunits, D_1 (purple) D_2 (blue) D_3 (brown) and D_4 (green), coat protein (grey) and internal scaffolding protein (peach) in the asymmetric unit. The locations of the second site suppressors are indicated with black dots. (C) The primary structure of the first α-helices from bacteriophages α3, G4, øX174, *øX174ΔD7*, and *øX174ΔD9*.

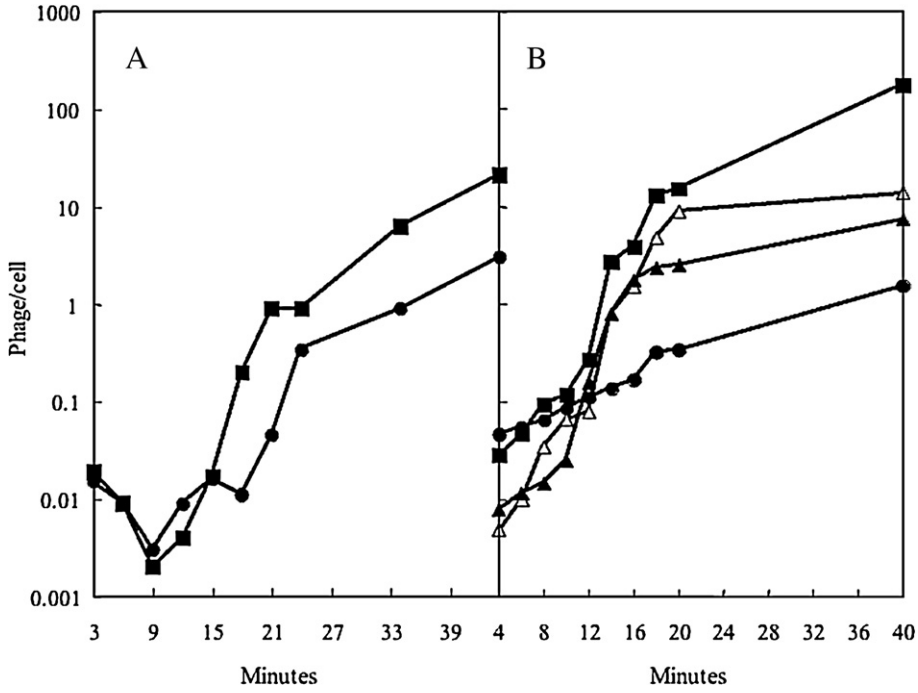

Fig. 2. Growth kinetics conferred by N-terminal deletion external scaffolding proteins. (A) Complementation of *øX174 nullD* by the cloned wild-type D (squares) and Δ*D7* (circles) genes. (B) Growth kinetics of the wild-type øX174, (closed squares), *øX174ΔD7* (circles), *su*(Δ*D7*)*PR2*/Δ*D7*(closed triangles), and *su*(Δ*D7*)*F-144*/Δ*D7* (open triangles).

dropped between 2–4 orders of magnitude at 26 °C and 42 °C. Plaque formation at the temperature extremes for both phages, as well as the small plaque *øX174ΔD7* phenotype at 33 °C, was efficiently rescued in cells expressing a cloned wild-type gene, demonstrating that the D protein deletions, not the missense mutation in gene C, were both necessary and sufficient to account for the defective phenotypes.

The kinetics of *øX174ΔD7* progeny production was analyzed in lysis-deficient cells (Fig. 2B). In these and all kinetic experiments, infections were synchronized as described in Material and methods and phage were pre-attached to cells. The wild-type curve has a short but pronounced lag phase followed by a rapid rise in progeny production (squares). The lag phase in this experiment conducted with wild-type øX174 is considerably shorter than that observed for the *nullD* mutant complemented with wild-type D protein (Fig. 2A, squares). This most likely reflects differences in host cell physiology, which would be affected by the use of antibiotic media and the expression of a phage protein from a high copy number plasmid. In this and other experiments conducted with the *øX174ΔD7* strain, it was difficult to precisely identify a lag phase (circles). While it is possible that the deletion of the first seven amino acids allows slow and constant assembly, the small differences between starting and ending titers most likely obfuscates detecting the lag phase within the curve. No virions were produced in *øX174ΔD9* infected even after 40 min of incubation (data not shown).

The differential yields between the wild-type and *øX174ΔD7* infections are accentuated when the proteins are expressed from viral genomes compared to the complementation studies, in which the external scaffolding proteins are expressed from the plasmids. Neither the overlap between genes C and D or the RBS for gene D were altered in producing the *øX174ΔD7* strain. However substitutions between the RBS and the start codon were introduced. Nucleotide changes in this region are known to affect protein levels in prokaryotic systems (de Smit and van Duin, 1990). To determine whether mutant D protein levels were altered in the *øX174ΔD7* strain, relative protein levels were investigated by examining whole cell lysates of infected cells by SDS PAGE. As can be seen in Fig. 3A, the amount of D protein, relative to other phage proteins, detected in *øX174Δ7* infected cells is lower compared to the wild-type control. To quantify these differences, the gel was analyzed for band intensity and area using NIH ImageJ software and the relative ratios of D protein were determined vis-à-vis proteins F and G. The results of this analysis indicate that the mutant D protein is expressed at approximately 15% of wild-type levels.

Characterization of particles produced in øX174ΔD7 and ΔD9 strains

Although external scaffolding protein levels are reduced in the *øX174ΔD7* strain, this reduction does not fully explain the defective phenotype. External scaffolding protein levels are 15% of wild-type, but virion yield is reduced more than two orders of magnitude. To investigate other possible assembly defects, extracts from *øX174ΔD7* and wild-type infected cells were generated and analyzed by rate zonal sedimentation. Initially, gradient and centrifugation parameters were designed to investigate particles with S values between 70–114 (Fig. 4A), the region of the gradient in which virions (114 S), procapsids (108 S) and degraded procapsids (70 S) are detected. Unlike the extracts from wild-type infected cells, virions and degraded procapsids were not detected by spectroscopy in mutant extracts, suggesting that a morphogenetic block occurs early in the assembly pathway and/or viral proteins are being siphoned off of the pathway.

To examine the production of the early intermediates with S values less than 50, lysates were again examined by rate-zonal sedimentation. However, after centrifugation, fractions were examined by SDS-PAGE as the small S values of the early assembly intermediates overlap with host cell complexes and large proteins making detection by spectroscopy unreliable. In extracts from *øX174ΔD7* infected cells (Fig. 4B) only 9S particles, consisting of coat protein pentamers, were observed. The presence of 9S particles differs from what is typically observed in *nullD* infected cells, in which assembly is arrested after the formation of the 12S* assembly intermediate (Fig. 1), before the first D protein mediated step in the pathway. As expected, very few small assembly intermediates were observed in the wild-type extracts as most structural proteins are incorporated into virions (Cherwa et al., 2008).

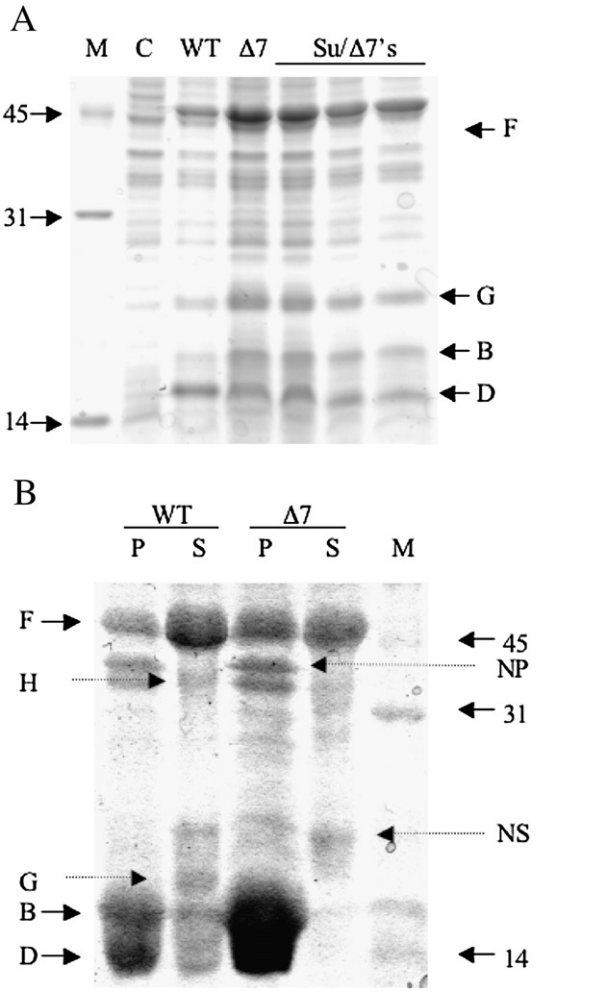

Fig. 3. Protein expression in *øX174ΔD7* and *su/øX174ΔD7* infected cells. (A) Whole cell lysates of wild-type, *øX174ΔD7* and *su/øX174ΔD7* infected cells. Lane M: molecular weight marker. Lane C: uninfected cells. (B) Pellet (P) and soluble (S) fractions from wild-type and particles synthesized in wild-type and *øX174ΔD7* infected cells. Viral proteins are indicated by letters on the left of the figure: F, viral coat protein; H, minor spike protein: G, major spike protein, B internal scaffolding protein, D, external scaffolding protein. The host protein bands labeled NS (*N*ormalization band for *S*upernatant fraction) and NP (*N*ormalization band for *P*ellet fraction) were used to normalize for differences that may have arisen during sample preparation. The exact identity of these host cell proteins is unknown. Lane M: molecular weight marker.

The low yield of large particles and the accumulation of a particle that occurs before the first D protein mediated step in that pathway suggest that the deletion proteins may be siphoning off intermediates from the pathway. To examine this possibility, soluble extracts and pellets from *øX174ΔD7* and wild-type infected cells were examined by SDS-PAGE (Fig. 3B). In extracts from mutant infected cells, the ratio of coat protein found in soluble and pellet fractions differs from the wild-type control, in which more coat protein in found in the soluble fraction. To quantify these differences, the gel in Fig. 3B was analyzed for band intensity and area using NIH ImageJ software. The host protein bands labeled NS (*N*ormalization band for *S*upernatant fraction) and NP (*N*ormalization band for *P*ellet fraction) were used to normalize for differences that may have arisen during sample preparation. The exact identity of these host cell proteins is unknown. After normalization, the coat protein supernatant:pellet ratios for the wild-type and mutant samples were determined to be 1.4 and 0.6, respectively. Thus, most of the coat protein in mutant infected cells is found in the insoluble fraction. It is unlikely that reduced levels of the mutant external scaffolding protein alone causes coat protein aggregation as the complete absence of external scaffolding proteins leads to the accumulation of the soluble 12S* intermediate (Cherwa et al., 2008). The coat protein in the soluble fraction most likely represents the unassembled 9S particles observed in Fig. 4B and any virions or defective large particles that may have formed. Since virion production is extremely low, approximately two orders of magnitude below wild-type (Fig. 2B), and large defective particles were not detected in mutant infected cells (Fig. 4A), the contribution of coat protein from these particles is most likely low.

Second site suppressors of the øX174ΔD7 defect map to the coat and external scaffolding protein

Although the *øX174ΔD7* temperature and cold-sensitive phenotypes are leaky, putative second site suppressors could be isolated as large plaque formers. Unlike the parental mutant, the putative suppressors plate with efficiencies near 1.0 at the temperature of isolation (Table 1) and plaque size is dramatically increased at 33 °C. Seven genetically distinct suppressors were isolated and appear to fall into two classes. The four members of the first class map between the RBS and start codon of gene D, a region that can also confer amino acid substitutions in the primary structure of protein C. However, the nucleotide change in one of these strains, *su*(*ΔD7*)*PR3*/*ΔD7* is silent in gene C, an AAG codon being changed to AAA. Thus, it is more likely that the suppressors in this region are altering the expression of the gene D. Whole cell lysates of infected cells were examined by SDS PAGE (Fig. 3A). To quantify differences in relative protein levels, the gel was analyzed for band intensity and area using NIH ImageJ

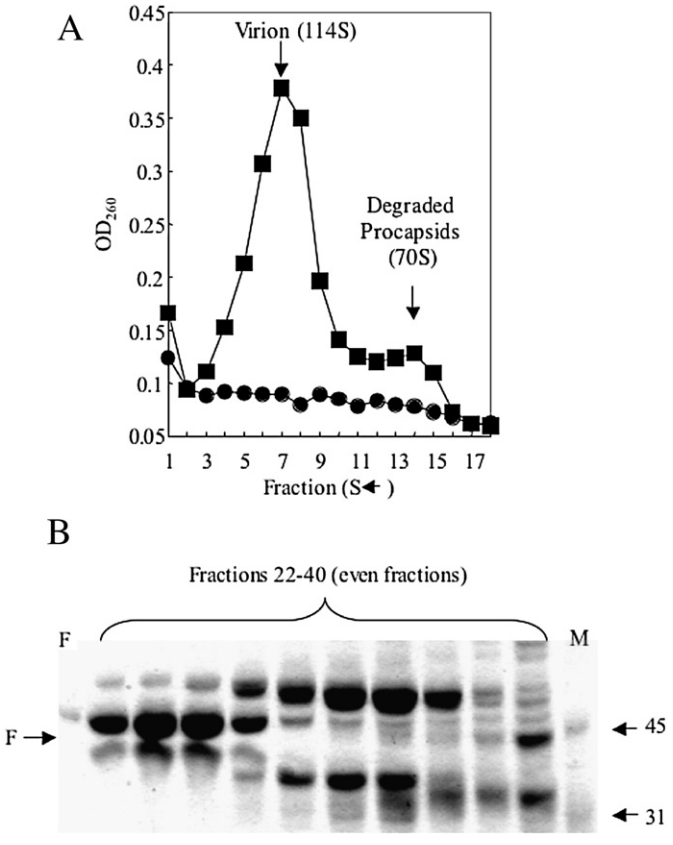

Fig. 4. Particles generated by wild-type and *øX174ΔD7*. (A) Large particles synthesized in wild-type (squares) and *øX174ΔD7*(circles) infected cells. Fraction one represents the bottom of the gradient. (B) Small particles synthesized in *øX174ΔD7* infected cells. Lane F: purified coat protein used as a marker. Lanes fractions 22–40 (even fractions): fractions from the gradient in which coat protein was detected, corresponding to the 9S region of the gradient. Lower numbered fractions represent faster sedimenting particles. The other bands are from host cell proteins. Lane M: molecular weight markers.

Table 1
Plating efficiencies[a] of the *øX174ΔD7* and suppressing strains

Strain	26 °C	33 °C	42 °C	Suppressor location
Wild-type øX174	1.0	1.0	1.0	
øX174ΔD7	10^{-3}	1.0	10^{-3}	
su(ΔD7)PR-1/ΔD7[b]	0.2	1.0	1.0	Nucleotide 387 T→C→G
su(ΔD7)PR-2/ΔD7	0.2	0.8	1.0	Nucleotide 384 G→T
su(ΔD7)PR-3/ΔD7	0.1	0.9	1.0	Nucleotide 384 G→A
su(ΔD7)PR-4/ΔD7	0.04	1.0	0.9	Nucleotide 387 T→C→T
su(ΔD7)F144/ΔD7	0.4	0.5	1.0	Coat protein a. a. 144 T→A
su(ΔD7)F238/ΔD7	0.4	1.0	10^{-3}	Coat protein a. a. 238 M→V
su(ΔD7)D111/ΔD7	0.6	1.0	0.8	D protein a. a. 111 V→L

[a] Efficiency of plating is defined as the assay titer/most permissive titer.
[b] Suppressor nomenclature: PR designates "putative regulatory", and is used for those suppressors mapping between the RBS and start codon of the 5′ deletion D gene. In those cases where the original nucleotide was changed in creating the Nde I site, three nucleotides are reported, the wild-type nucleotide, the change to create the restriction site, and the change that resulted in the suppressing phenotype. Suppressors within the coat and external scaffolding proteins are distinguished with the letter, D or F for external scaffolding or coat protein, followed by the altered amino acid in the primary structure. Thus, F144 indicates a mutation in amino acid 144 of the coat protein.

software and the relative ratios of D protein were determined vis-à-vis proteins F and G. Mutant D protein levels are higher in the suppressor strains but still fall below wild-type levels. For the suppressor strains, the amount of detectable D protein ranged from approximately 25–35% of wild-type levels. The level in the parental strain was approximately 15%. Thus, the suppressors may increase D protein levels by a factor of 2.

Members of the second class of suppressors are located in the coat and external scaffolding protein (Table 1; Fig. 1B). To verify the identity of the suppressors, recombination rescue experiments were performed. A wild-type and a suppressor coat protein gene were isolated by TA cloning. Cells harboring these clones were then infected with *øX174ΔD7* at 33 °C and the resulting progeny were assayed for the ability to grow at 26 °C, a restrictive temperature. The restrictive plating frequency for progeny propagated in the host carrying the suppressor gene was 0.24, a value three orders of magnitude higher than that obtained from the progeny propagated in cells carrying the clone of the wild-type gene. The *su(ΔD7)F144* mutation was also placed in a wild-type background. Alone, this mutation confers no detectable phenotype.

Growth curve experiments were conducted with the suppressor strains, as can be seen in Fig. 2B, the suppressors (open and closed triangles) appear to restore a pronounced lag phase, as seen in wild-type curves. Although final yields are one of order of magnitude above those of the parental strain, they still fall an order of magnitude below wild-type levels. However, the level of virion produced in the suppressor strains is more consistent with the expression levels of the mutant external scaffolding protein. Extensive efforts were made to isolate mutations that restore viability to the *øX174ΔD9* strain but none were recovered. If they occur, they occur at a frequency less than 1.0×10^{-9}, indicative that multiple mutational events would be required.

Discussion

The kinetics of *in vivo* bacteriophage production occurs rapidly after an initial lag phase. Two factors contribute to the length of the lag phase: temporal gene expression and the rate-limiting reaction of nucleation complex formation. As there is no temporal gene expression during a øX174 infection, the lag phase seen in synchronized øX174 infections is most likely a function of obtaining the critical concentrations of assembly intermediates and proteins required to drive the formation of nucleation complexes. After nucleation complexes are formed, assembly components add rapidly ensuring that morphogenesis goes to completion (Prevelige et al., 1993). The results of past studies with chimeric external scaffolding and internal scaffolding protein independent strains demonstrate that the length of the lag phase can be correlated to obtaining external scaffolding protein critical concentrations (Chen et al., 2007; Uchiyama et al., 2007; Uchiyama and Fane, 2005). With strains that no longer require the internal scaffolding protein, the over expression of the external scaffolding protein is capable of shortening lag phases, allowing virion formation to occur before programmed cell lysis. With the chimeric external scaffolding strains, lag phases were shortened by the introduction of coat protein substitutions at the three-fold axes of symmetry or by expressing the chimeric protein concurrently from the viral genome and a plasmid.

The chimeric proteins were made by interchanging the first α-helices of the G4 and øX174 proteins. The C-terminal residues of these helices are mostly conserved but there is considerable divergence between the N-terminal seven amino acids (Fig. 1C). To further characterize the morphogenetic role of the diverged region, øX174 N-terminal deletion proteins were generated and characterized for their ability to support morphogenesis. As seen with the chimeric proteins, the expression of the deletion protein from a pre-induced plasmid resulted in a longer lag phase.

The deletion proteins were also expressed from the viral genome. The molecular basis of the *øX174Δ7*mutant phenotype is complex. Mutant protein levels are lower than wild-type, which could affect procapsid nucleation, and the protein appears to remove assembly intermediates from the productive pathway. Removal is not a function of lower external scaffolding protein levels as the complete absence of external scaffolding proteins leads to the accumulation of the soluble 12S* intermediate (Cherwa et al., 2008). The 12S* particle is the last intermediate before the first D protein mediated step and occurs after the formation of the 9S particle, which was detected in mutant infected cells. Thus, it is most likely that 12S* particles are being removed from the pathway in a reaction that competes with procapsid formation. *In vivo* kinetics experiments only measure the production of infectious progeny, not the production of off-pathway aberrant structures, which can be detected by *in vitro* experiments (Parker et al., 1998; Stray et al., 2005). Thus, it is not possible to determine whether possible off-pathway reactions occur at the same rate as productive procapsid formation. Correlations between increased *in vitro* assembly rates and the production of aberrant off pathway particles have been noted in the P22 system (Parker et al., 1998).

Second-site suppressor strains, which relieved the poor growth phenotype of the *øX174ΔD7* strain were identified. Although multiple stocks were used and most suppressors were independently isolated more than once, the suppressors of the chimeric protein, primarily located in a large α-helix in the viral coat protein, were not represented in this new pool of mutations. Alterations in this coat protein helix may be required to interact with the altered amino acid residues found in the chimeric strain (Uchiyama and Fane, 2005; Uchiyama et al., 2007). However, this may not be a viable mechanism of suppression if the N-terminal region of the helix is altogether missing.

The suppressors of the N-terminal deletion protein appear to fall into two classes. Members in the first class are located between the RBS and the start codon of the 5′ deletion gene. Changes in these regions are known to affect the efficiency of prokaryotic translation (de Smit and van Duin, 1990). Mutant D protein levels produced by suppressor strains appear to be higher parental strain, but still fall below wild-type levels. The growth curves of these suppressor strains resemble wild-type øX174 curves. The increased level of external scaffolding protein could elevate the number of productive nucleation events and increase yields to a level facilitating the identification of a distinct lag phase. However, yields are still reduced by one order of magnitude, suggesting that other assembly defects, which may still involve nucleation, are occurring, which is consistent with the pleotropic nature of the mutant.

The second class of suppressors may be acting on the level of protein–protein interactions. As can be seen in Fig. 1B, the suppressing amino acids located in the external scaffolding protein reside in the coat-external scaffolding protein interface. In the atomic structure of the procapsid (Dokland et al., 1999, 1997), this residue in the D_1 and D_2 subunits make direct contact with coat protein residues 152 and 144, respectively. Residue 144 was also identified as a suppressor. The coat protein suppressor located at residue 238 makes direct contact with the internal scaffolding protein. Coat-internal scaffolding protein interactions have been shown to influence subsequent interactions with the external scaffolding protein, conferring resistance to dominant negative external scaffolding mutations (Cherwa et al., 2008).

These interface suppressors could act by lowering the critical concentration of the deletion proteins required for nucleation, which would in turn elevate yields and facilitate lag phase detection. Alternatively, the suppressors could prevent the removal of assembly intermediates from the pathway. These two mechanisms of suppression are not mutually exclusive phenomena. By lowering the critical concentration required for proper procapsid nucleation, less material is available for an off pathway reaction. Similarly, blocking an aggregation pathway would elevate the scaffolding protein and intermediate levels available for productive assembly.

Materials and methods

Phage plating, media, buffers, stock preparation, generation of single stranded (ss) DNA, replicative form (RF) DNA, DNA isolation, and rate zonal sedimentation and protein electrophoresis

The reagents, media, buffers, and protocols have been previously described (Fane and Hayashi, 1991). Rate zonal sedimentation and protein electrophoresis protocols are identical to those previously published (Uchiyama and Fane, 2005).

Bacterial strains and plasmids

The *Escherichia coli* C strains C122 (*sup*^{0}) and BAF30 (*recA*) have been described previously (Fane and Hayashi, 1991; Burch et al., 1999). The C900 strain contains the host *slyD* mutation, which confers resistance to E protein-mediated lysis (Roof et al. 1994). To construct the plasmids pDΔ7 and pDΔ9, which express N-terminal deletion D proteins, an Nco I site, containing a start codon, had to be placed in either codon 7 or 9. This was done by using mutagenic upstream primers in PCR reactions. The D gene in plasmid pND (Cherwa et al., 2008) served as a template. The downstream primer annealed to the multi-cloning site of the pND vector. PCR products were digested with Nco I and Hind III and ligated into pSE420 (Invitrogen) digested with the same enzymes. Gene expression is under *lac* control.

Construction of the øX174ΔD7 and øX174ΔD9 strains and the isolation of second-site suppressors of øX174ΔD7

Oligonucleotide-mediated mutagenesis, conducted as previously described (Fane et al., 1993), was used to generate the parental strain from which the deletion strains were derived. The mutagenic oligonucleotide was designed to place an Nde I site spanning the start codon, an ochre mutation in codon three, and a second Nde I site spanning codon seven. It was annealed to øX174 ssDNA that had been previously modified by the addition of a silent Pvu I site downstream of gene D. After *in vitro* DNA synthesis, the DNA was transfected into BAF30 expressing the wild-type D protein. Plaques were stabbed into two indicator lawns. Mutant phages were identified by a complementation dependent phenotype.

To generate the *øX174ΔD7* strain, replicative form (RF) DNA was generated as previously described (Burch et al., 1999) and cut with Nde I. After ligation, DNA was transfected into BAF30 pND. Plaques were stabbed into two indicator lawns. Mutant phages were identified by a complementation dependent phenotype. To generate the *øX174 ΔD9* strain, øX174 DNA with the silent Pvu I site was used as a template to amplify DNA containing an Nde I site spanning codon 9, which was introduced by the upstream primer. After amplification, the PCR product was digested with Nde I and Pvu I and ligated into *øX174ΔD7* RF DNA digested with the same enzymes. The genotypes of all strains were verified by a direct sequence analysis.

Kinetic experiments (viral growth curves)

C900 cells, containing the host *slyD* mutation, which confers resistance to E protein-mediated lysis (Roof et al., 1994), were grown to a concentration 1×10^8 cells/ml in TK media (1.0% tryptone, 0.5% KCl). Cells were washed twice with HFB buffer (Fane and Hayashi, 1991) before being resuspended in HFB buffer with 10 mM $MgCl_2$ and 5.0 mM $CaCl_2$. 0.9 ml of cells were mixed with 0.1 ml phage at a concentration of 1.0×10^7 ø/ml. Mixtures were incubated at 37 °C to allow phage attachment. Cells with attached phage were concentrated by centrifugation. At $t=0$, pellets were resuspended in 1.0 ml pre-warmed TK media at 33 °C. For time points, 50 µl aliquots were removed and placed into 0.5 ml iced $CHCl_3$-saturated HFB containing 2.0 mg/ml hen egg white lysozyme.

Acknowledgments

The authors thank James Cherwa for discussion. This research was supported by National Science Foundation grant MCB 054297 to B.A.F.

References

Burch, A.D., Fane, B.A., 2000. Foreign and chimeric external scaffolding proteins as inhibitors of *Microviridae* morphogenesis. J. Virol. 74 (20), 9347–9352.
Burch, A.D., Ta, J., Fane, B.A., 1999. Cross-functional analysis of the *Microviridae* internal scaffolding protein. J. Mol. Biol. 286 (1), 95–104.
Chen, M., Uchiyama, A., Fane, B.A., 2007. Eliminating the requirement of an essential gene product in an already very small virus: scaffolding protein B-free oX174, B-free. J. Mol. Biol. 373 (2), 308–314.
Cherwa Jr., J.E., Uchiyama, A., Fane, B.A., 2008. Scaffolding proteins altered in the ability to perform a conformational switch confer dominant lethal assembly defects. J. Virol. 82 (12), 5774–5780.
de Smit, M.H., van Duin, J., 1990. Secondary structure of the ribosome binding site determines translational efficiency: a quantitative analysis. Proc. Natl. Acad. Sci. U. S. A. 87 (19), 7668–7672.
Dokland, T., McKenna, R., Ilag, L.L., Bowman, B.R., Incardona, N.L., Fane, B.A., Rossmann, M.G., 1997. Structure of a viral procapsid with molecular scaffolding. Nature 389 (6648), 308–313.
Dokland, T., Bernal, R.A., Burch, A., Pletnev, S., Fane, B.A., Rossmann, M.G., 1999. The role of scaffolding proteins in the assembly of the small, single-stranded DNA virus phiX174. J. Mol. Biol. 288 (4), 595–608.
Fane, B.A., Hayashi, M., 1991. Second-site suppressors of a cold-sensitive prohead accessory protein of bacteriophage øX174. Genetics 128 (4), 663–671.
Fane, B.A., Prevelige Jr., P.E., 2003. Mechanism of scaffolding-assisted viral assembly. Adv. Protein Chem. 64, 259–299.
Fane, B.A., Shien, S., Hayashi, M., 1993. Second-site suppressors of a cold-sensitive external scaffolding protein of bacteriophage øX174. Genetics 134 (4), 1003–1011.
Fane, B.A., Brentlinger, K.L., Burch, A.D., Hafenstein, S.L., Moore, E., Novak, C.R., Uchiyama, A., 2006. øX174 et al, In: Calendar, R. (Ed.), Second ed. The Bacteriophages. Oxford Press, London, pp. 129–145.
Goldstein, R., Lengyel, J., Pruss, G., Barrett, K., Calendar, R., Six, E., 1974. Head size determination and the morphogenesis of satellite phage P4. Curr. Top. Microbiol. Immunol. 68, 59–75.
King, J., Casjens, S., 1974. Catalytic head assembling protein in virus morphogenesis. Nature 251 (5471), 112–119.
Parker, M.H., Casjens, S., Prevelige Jr., P.E., 1998. Functional domains of bacteriophage P22 scaffolding protein. J. Mol. Biol. 281 (1), 69–79.
Prevelige Jr., P.E., Thomas, D., King, J., 1993. Nucleation and growth phases in the polymerization of coat and scaffolding subunits into icosahedral procapsid shells. Biophys. J. 64 (3), 824–835.
Roof, W.D., Horne, S.M., Young, K.D., Young, R., 1994. SlyD, a host gene required for øX174 lysis, is related to the FK506-binding protein family of peptidyl-prolyl *cis-trans*-isomerases. J. Biol. Chem. 269 (4), 2902–2910.
Stray, S.J., Bourne, C.R., Punna, S., Lewis, W.G., Finn, M.G., Zlotnick, A., 2005. A heteroaryldihydropyrimidine activates and can misdirect hepatitis B virus capsid assembly. Proc. Natl. Acad. Sci. U. S. A. 102 (23), 8138–8143.

Tonegawa, S., Hayashi, M., 1970. Intermediates in the assembly of phi X174. J. Mol. Biol. 48 (2), 219–242.
Uchiyama, A., Fane, B.A., 2005. Identification of an interacting coat-external scaffolding protein domain required for both the initiation of phiX174 procapsid morphogenesis and the completion of DNA packaging. J. Virol. 79 (11), 6751–6756.
Uchiyama, A., Chen, M., Fane, B.A., 2007. Characterization and function of putative substrate specificity domain in microvirus external scaffolding proteins. J. Virol. 81 (16), 8587–8592.
Wang, S., Palasingam, P., Nokling, R.H., Lindqvist, B.H., Dokland, T., 2000. In vitro assembly of bacteriophage P4 procapsids from purified capsid and scaffolding proteins. Virology 275 (1), 133–144.